Shao, L.-H.; Biener, J.; Jin, H.-J.; Biener, M.M.; Baumann, T.F.; Weissmueller, J.:

Electrically Tunable Nanoporous Carbon Hybrid Actuators

In: Advanced Functional Materials (2012) Wiley

DOI: 10.1002/adfm.201200245

Electrically tunable carbon aerogel hybrid actuator

L.-H. Shao,[1,2] J. Biener,[3] H.-J. Jin,[2,4] T. F. Baumann,[3] J. Weissmüller[1,5]

1 Institut für Werkstoffphysik und -Technologie, Technische Universität Hamburg-Harburg, Hamburg, Germany
2 Institut für Nanotechnologie, Karlsruher Institut für Technologie, Karlsruhe, Germany
3 Lawrence Livermore National Laboratory, California, USA
4 Institute of Metal Research, Shenyang National Laboratory for Materials Science, Chinese Academy of Sciences, Shenyang, P.R. China.
5 Institut für Werkstoffforschung, Werkstoffmechanik, Helmholtz-Zentrum Geesthacht, Geesthacht, Germany

Within recent years, various novel nanomaterials have been tested for possible application as actuators. Here we report on an actuator based on a hybrid carbon-aerogel electrolyte material. Carbon aerogels are light-weight, low-cost materials with extremely high surface area. They form macroscopic monolithic bodies with three-dimensional hierarchical architectures. In contrast to lower dimensional nanomaterials, carbon aerogels can be loaded in compression. The hybrid material is formed by imbibing the pore space with aqueous electrolyte. We found that the strain amplitude is proportional to the BET mass specific surface area, with reversible volume strain amplitudes up to the exceptionally high value of 6.6%. The mass-specific strain energy density, estimated from the Young's modulus measured in uniaxial compression, compares favorably to reported values for piezoceramics and for nanoporous metal actuators.

1. Introduction

Actuator materials, which can reversibly change their dimensions upon converting the electrical, thermal, chemical or magnetic energy to mechanical energy, have been studied for many years, such as piezoelectric, electrostrictive ceramics and magnetostrictive actuators [1]. As a rule, the applications of these materials are restricted by the need for high voltage and/or magnetic fields [2]. There is also currently considerable interest in electrochemically driven actuator systems for applications ranging from microswitches to artificial muscles [3,4]. Considerable experimental and theoretical progress has been made in understanding charge-induced reversible strain effects in nanomaterials, and various actuator applications have been suggested for nanoporous noble metals [4-6], carbon nanotubes (CNT) [3,7-9] and graphene [10,11]. However, applications are currently hampered by high materials costs and the fact that typical CNT arrays and graphene are poorly suited for loading in compression. It is therefore of interest to search for alternative materials that combine mechanical and chemical stability with low cost, such as activated carbons [12].

The first observations of reversible dimensional changes of a porous carbon electrode have been published as early as 1972 [13]. Two decades ago, this work was continued with different carbon and graphite electrodes [14,18]. In previous work on the potential of zero charge of carbon aerogels (CAs), we reported charge-induced reversible dimensional changes of CA electrodes [19]. Here, we report on the electrochemical-mechanical properties of CAs, and demonstrate that large volume strain values (up to 6.6%) and mass-specific energy densities can be realized.

CAs are unique porous materials that exhibit numerous exceptional properties such as controllable mass densities, contiguous open porosity, large specific surface area (up to 3200 m^2/g), and high electrical conductivity [20,21]. The skeletal structure of the material consists of interconnected, sub-micron size particles with an inner nanoscale pore structure which exposed nearly all carbon atoms to an interface [19]. Their properties make CAs promising candidate materials for supercapacitors, rechargeable batteries, advanced catalyst supports,

adsorbents and chromatographic packing thermal insulators [22-24].

The pore space of nanoporous materials can be filled with liquid electrolyte, for instance, an aqueous salt solution or an ionic liquid. The material then consists of two phases with very different properties (e.g., solid versus liquid, electron conductive versus ion conductive) which are interlaced at the nanoscale. Such hybrid materials may exhibit novel functional properties that are not observed in the isolated phases. This has recently been demonstrated with a hybrid material interlacing nanoporous metal with perchloric acid, which enabled a reversible electric control of the mechanical strength and flow stress [25]. Here, we apply a similar concept to CAs. We show that the CA-based hybrid material can be made to expand and contract reversibly upon application of an electric bias between the two conduction channels, ionic and electronic. The strain amplitudes and strain energy densities exceed those of conventional actuator materials. Thus, the material may be a contender for application as a low cost actuator.

2. Results and Discussion

In this work, we used the CA samples with four different mass-specific BET (Brunauer-Emmett-Teller) surface areas, namely 440, 1490, 2800 and 3032 m^2/g [19]. An aqueous solution of NaF (0.7 M) was chosen as the electrolyte. Fluoride anions are known to show little specific adsorption on CA surfaces near the pzc [26]. This allows us to focus on pure capacitive double-layer charging with minimum contributions from pseudocapacity. The hybrid material is formed by imbibing the pore space with aqueous electrolyte. The imbibition is spontaneous, though with a slow kinetics, see below.

The conditioning of a fresh CA-hybrid sample during continuous cycling in 0.7 M NaF solution (−0.7 V to 0.9 V, 1 mV/s) is shown in Figure 1. The strain amplitude slowly increases with time for approximately one day, and then stays constant. As discussed in our previous work [19], ‘fresh’ samples tend to float upon their first contact with electrolyte, indicating that a major pore fraction is not immediately wetted. In agreement with that observation, the capacity as well as the strain amplitude in in-situ dilatometry are initially small and increase during the first cycles. After repeated cycling both values stabilize, and the samples do no longer float. This was taken as evidence that the electrolyte tends to wet the pores spontaneously, but with a slow kinetics. In the present study, the strain amplitude finally reached nearly 1%, considerably larger than that in the scans with smaller potential window as described previously.

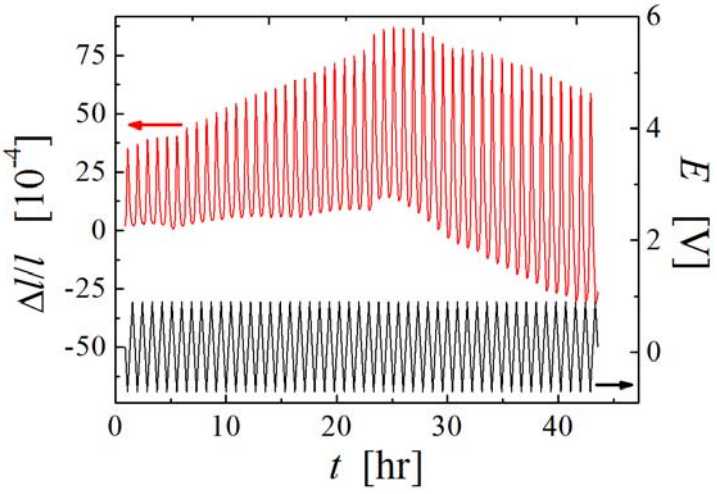

Fig.1 Relative length change, $\Delta l/l$, in response to the variation of the electrode potential, E, with time (t). Potential ranges from −0.7 to 0.9 V. Electrolyte is aqueous 0.7 M NaF, scan rate is 1 mV/s.

Figure 2 compares charging current and length change vs. applied potential for various scan rates. The length change (Fig. 2b) was recorded simultaneously with the cyclic voltammograms (CVs) shown in Fig. 2(a). Expansion of the CA-hybrid material is observed for negative potentials (electron accumulation), and contraction for positive potentials (hole accumulation). This behavior agrees well with the result of a density functional theory (DFT) study on charge-induced dimensional changes of graphite [27]. The charge-induced strain of CNTs depends on the chirality and the diameter [28,29]. For example, Verissimo-Alves et al. found with metallic CNTs and graphene, upon increasing hole densities, the lattice constant initially contracts, reaches a minimum, and then starts to expand. Semiconducting CNTs with small diameters ($d \leq 20$ Å) always expand upon hole injection, and semiconducting CNTs with large diameters ($d \geq 20$ Å) display a behavior intermediate between those of metallic and large-gap CNT's [28]. More recently, Rogers and Liu reported a parabolic relationship between the strain and potential of monolayer graphene, and concluded that the electrostatic forces in the double layer dominate the actuation mechanism, as opposed to modified bond forces due to charge injection into the solid [30]. The varied points of view expressed in these studies highlight that the mechanism of charge-induced strain in carbon nanomaterials is poorly understood and requires further studies.

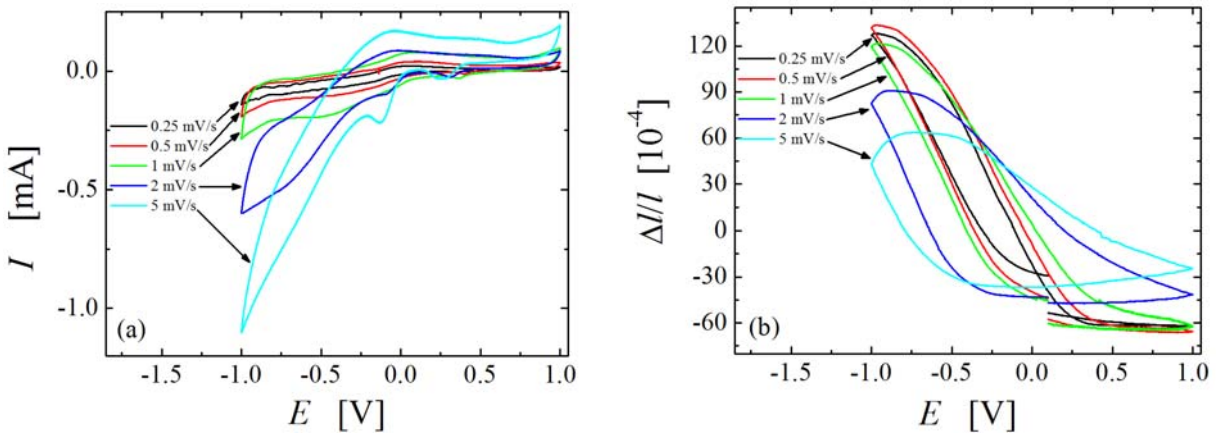

Fig. 2 Simultaneously recorded data for electrochemical and mechanical behaviour of a carbon aerogel hybrid actuator. Potential range is −1.0 to 1.0 V in 0.7 M NaF solution, results for different scan rates are shown. (a), Cyclic voltammograms (current I vs. electrode potential E). (b), Relative length change, $\Delta l/l$, vs. E.

We find that the strain amplitude depends only weakly on the potential scan rate as long as that rate does not exceed 1 mV/s. This suggests that the experiment probes saturation strain values under these conditions. In faster scans (Fig. 2 (b), the strain amplitude decreases with increasing scan rate. The effect of scan rate on the actuator response is summarized in Fig. 3. At low scan rates, very large strain amplitudes can be realized, but the strain amplitude slowly drifts thus indicating irreversible changes related to some plastic deformation of carbon aerogel and/or due to the electrochemical activation process (e.g., removing some contaminations at the surface of the sample) during the electrochemical scanning. Full reversibility of the length change is achieved at higher scan rates [5 mV/s, Fig.3(b)]. Thus, the irreversibility can be avoided under appropriate operation conditions.

Remarkably, the maximum strain amplitude emerges as 2.2%, which is very large. Furthermore,

the volume strain, which is three times the length change, emerges as 6.6%. Both strain values considerably exceed what has been reported with nanoporous metals so far [4,31]. The present values are also much larger than the strain amplitude of the most common stiff actuator materials, namely piezoceramics. Those substances exhibit strain amplitudes of 0.1-0.2% [32]. The typical carbon nanotube arrays, which have been suggested for actuation application, can only achieve 1% strain in aqueous electrolyte [3].

We note that the strain amplitude of 2.2 % value is consistent with the 2% maximum variation in basal plane dimension that is observed for graphite intercalation compounds [3]. This may highlight the parallels between double-layer charging at the metal-electrolyte interface and charge transfer between intercalated atoms and the graphite basal planes of an intercalation compound.

For actuation application, the reaction rate is an important parameter. The halftimes of the jumps in current and strain are 145 s and 165 s. Because of the limited sampling rate (10 s^{-1}) of the dilatometer, the time constant obtained from the charging curves is considered more accurate. Figure 3 (c) shows the frequency dependence of the amplitude (in the form of percentage of the maximum strain amplitude) during potential jumps. The strain amplitude at a frequency of 7 mHz is almost identical to that during slower switching, which is consistent with the response time given above. The characteristic frequency, ω_c, is also measured with 0.05 M NaF, which emerge as 2 mHz. And the values of ω_c are same with 1 M H_2SO_4 aqueous solution and with 1-butyl-3-methylimidazolium tetrafluoroborate (C8H15BF4N2), which is 15 mHz. These characteristic frequency values suggest that the reaction is faster within the solutions of higher electric conductivity [33,34].

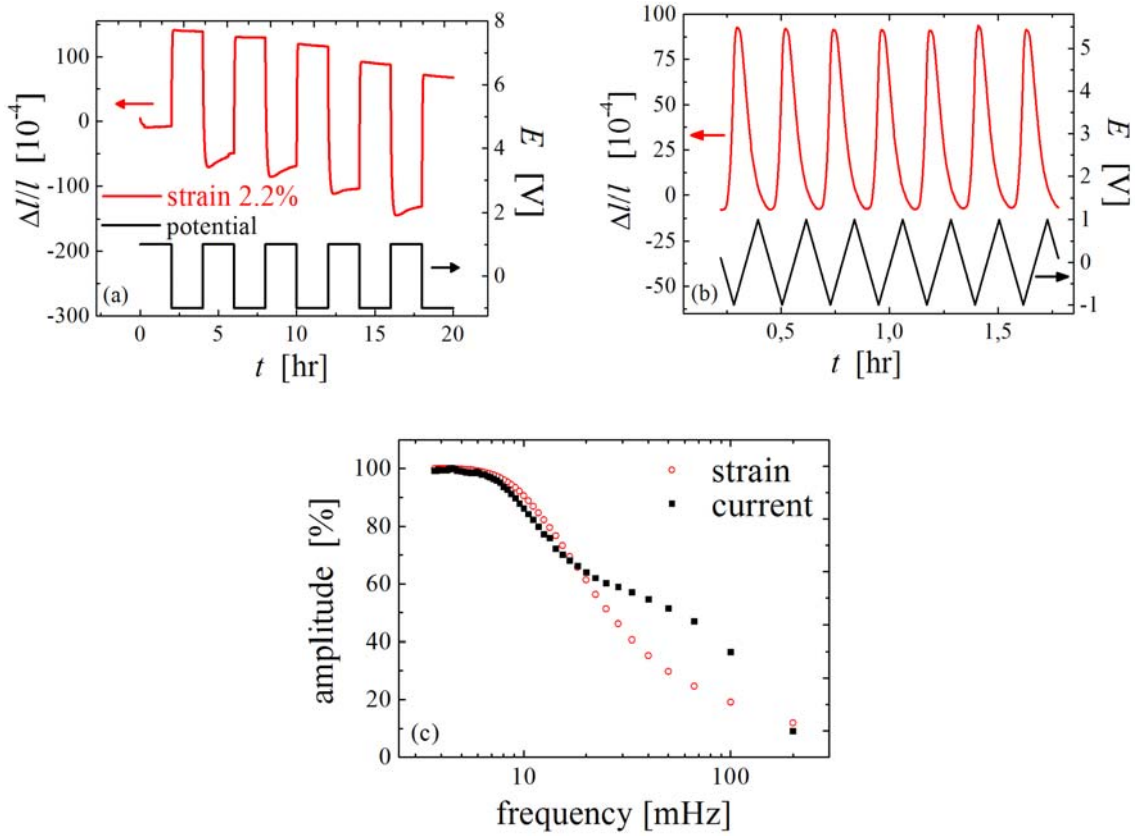

Fig. 3 In-situ dilatometry measurement of the CA hybrids with the potential range from −1.0 to 1.0 V in 0.7 M NaF solution. (a), strain $\Delta l/l$ in response to the potential E variation in the time (t-) domain. (b), strain $\Delta l/l$ in response to the potential E variation at the scan rate of 5 mV/s. Note the strain changes reversiblely. (c), frequency dependence of the amplitude (% means that the percentage of the maximum strain amplitude) during potential jumps (rectangular wave). Large squares (black): Amplitude of the charging curve. Small circles (red): Amplitude of the length change as measured in the dilatometer.

Figure 4 presents the strain amplitudes of CA-hybrid samples with different mass specific surface areas, α_M (namely 440, 1490, 2800 and 3030 m^2/g) in the potential range from −0.7 V to 0.9 V (dark triangle) and −1.0 to 1.0 V (red square), respectively. The plot shows a linear dependence of strain on the BET surface area, the slopes are 7.1×10^{-4} and 1.5×10^{-4} g/m^2, respectively. The sample with the highest mass-specific surface area, i.e. 3030 m^2/g, emerges the largest strain. The maximum strain amplitude changing linearly with the BET surface area suggests that all the carbon atoms are exposed to the electrolyte, which agrees well with the capacity measurement in our previous work [19].

It is well known that, in the electrochemical actuator systems, increasing the magnitude of the applied potential can increase the strain amplitude, which is also verified in this work. However, higher potential will induce electrolysis of water and generate bubbles on the sample surface. This would decrease the lifetime of the actuator. Therefore, the method of increasing the potential to obtain larger strain is limited. Strains of 0.1 - 1% have been reported based on film type single-wall carbon nanotube actuators. The multi-wall carbon nanotubes actuator shows strains up to 0.15% within a 4 V potential interval [35], where the potential is twice the potential window used in this work but resulting in a considerably smaller strain amplitude than our CA-hybrid samples.

With our material, except choosing the different potential range to get the corresponding strain, it is not only possible to keep the potential in a relatively smaller interval, but also to choose samples with different surface area to achieve a particular strain, which depends on the relations between strain and BET surface area as shown in Fig. 4.

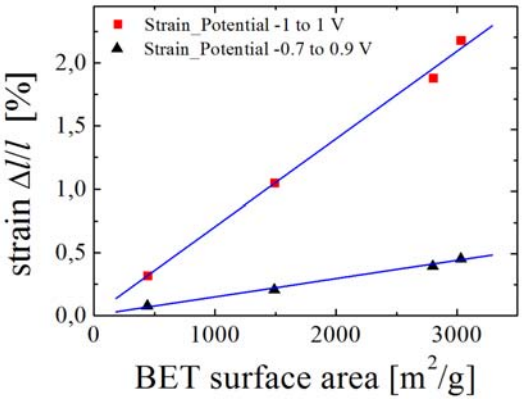

Fig. 4 In-situ scans with different CA-hybrid samples in 0.7 M NaF at the scan rate of 1 mV/s and in a potential range from − 0.7 V to 0.9 V (dark triangle) and − 1.0 to 1.0 V (red square), respectively.

An important parameter of an actuator is its work density, w. Assuming the actuator behaves like a linear elastic solid, the mass-specific strain energy density, w_M, is given as $w_M = ½ Y_{eff} \varepsilon^2_{max}/\rho$, where Y_{eff} is the effective macroscopic Young's modulus, ε_{max} is the maximum strain amplitude and ρ is mass density [31]. The effective macroscopic Young's modulus Y_{eff} was measured in compression on a testing machine [36] for miniature samples under controlled cross-head speed. The displacement of the cross-head was recorded, and empty runs produced a baseline used for correction the effects caused by the machine compliance. The engineering stress was determined as $\sigma = F/S_0$, where F is the force and S_0 is the initial area of sample cross section. The engineering strain ε is defined as $\delta l/l_0 \times 100\%$, where δl is the displacement of the sample upon compression and l_0 is the sample initial length. An example of a stress-strain curve obtained for a 3189 m^2/g sample is shown in Fig. 5. The strain range from 3% to 5% is used to calculate Y_{eff}, which emerges as 280 (± 2) MPa. Reported values for Y_{eff} of CA's are similar [37,38] or larger [39,40] than the present one. We thus estimate that 280 MPa is a conservative value for the effective stiffness that can be used to estimate the strain energy density. The result for w_M obtained in this way is 485 (± 3.5) J/kg with the values ε_{max} = 2.2% and ρ = 0.14 g/cm^3 [19], respectively.

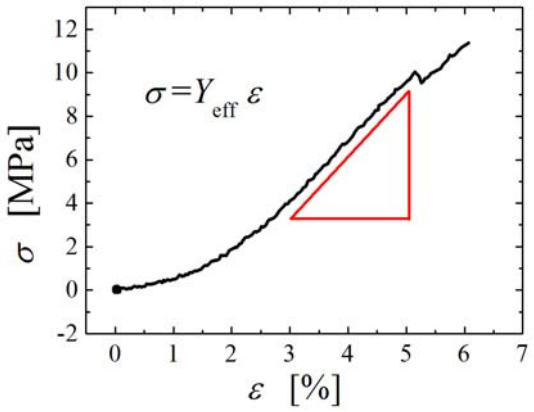

Fig. 5 Stress-strain curve of CA-hybrid sample measured by compression test.

Some characteristic figures of merit for different types of actuator materials are compared in Fig. 6. While the largest strain amplitudes are reached by dielectric elastomers [41] and by skeletal muscles [42], and the highest stiffness is observed for piezoceramics [32] and np metals [31], carbon aerogel hybrids show the largest mass-specific strain energy density. Furthermore, and as compared to the conventional actuation materials shown in the chart, carbon aerogels are distinguished by their low operating voltage. The significant drawback of CA's as actuators is their slow response. Yet, for applications that tolerate actuation times in the order of seconds, CA's may be a useful materials choice. Quite specifically, the combination of low voltage, large strain amplitude and high mass-specific strain energy density make carbon aerogel as an attractive, low cost material for the conversion of electric energy into mechanical work.

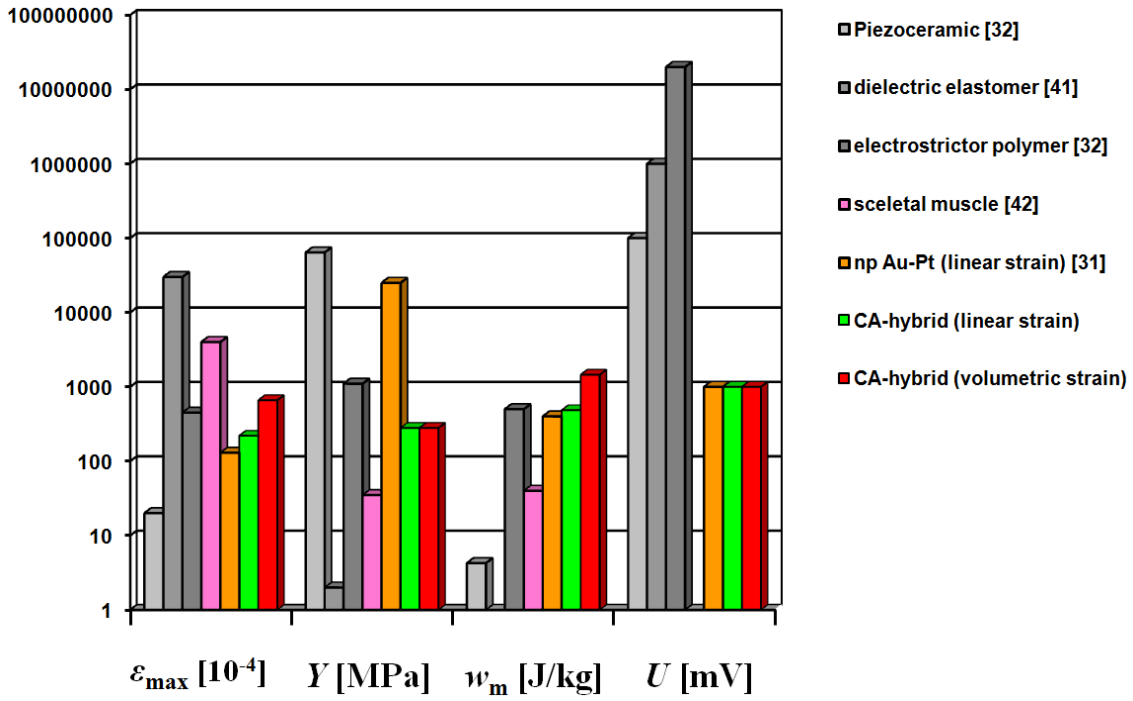

Fig. 6 Column chart plot of characteristics of various actuator materials. ε_{max}, maximum strain; Y, effective modulus; ω_m, mass-specific strain energy density; U, operating voltage for 100 μm actuator size.

3. Conclusions

We have reported an electrically tunable carbon aerogel hybrid actuator. The exceptionally large strain amplitude and high mass-specific strain energy distinguish the material as a candidate for use as a light-weight, low-cost actuator. The linear strain amplitude reaches 2.2% and, due to the isotropic materials structure, the volume strain is three times as high, 6.6%. Other nanoporous materials, such as Pt and Au, exhibit considerable lesser values of the strain amplitude and strain energy densities. In fact, the mass-specific strain energy density of the hybrid material even exceeds that of piezoceramics.

4. Experimental section

Sample Preparation. The carbon aerogel material was synthesized through the acid-catalyzed sol-gel polymerization of resorcinol with formaldehyde to produce organic gels that then are supercritically dried and pyrolyzed in an inert atmosphere. The details can be found in Refs. [19,20]. As the working electrode, we used a cuboid carbon aerogel sample with the dimension of $1\times1\times2$ mm^3. The same material was used as counter electrode but with an at least 5 times larger volume.

Electrochemical Measurements. The commercial dilatometer equipped with an in-situ electrochemical cell is otherwise identical to that described in Ref. [43]. Measurement procedures are analogous to Ref. [19]. Ultrapure 18.2 MΩcm grade water (Arium 611, Sartorius, Germany)

plus NaF or H_2SO_4 (Suprapur, Merck), was used to prepare the electrolytes. All experiments were performed at room temperature, using commercial Ag/AgCl reference electrodes (+200mV vs. a standard hydrogen electrode) in KCl solution (DRIREF-2, World Precision Instruments, Inc.).

Acknowledgements

[1] Stephen A. Wilson, Renaud P.J. Jourdain, Qi Zhang, et al. New materials for micro-scale sensors and actuators An engineering review. Materials Science and Engineering R 56 (2007) 1–129.

[2] Y.H. Yun, V. Shanov, Y. Tu, M. J. Schulz, S. Yarmolenko, S. Neralla, J. Sankar, S. Subramaniam. NanoLetters 6(4) (2006) 689–693

[3] R. H. Baughman, C. Cui, A. A. Zakhidov, Z. Iqbal, J. N. Barisci, G. M. Spinks, G. G. Wallace, A. Mazzoldi, D. De Rossi, A. G. Rinzler, O. Jaschinski, S. Roth, M. Kertesz. Science **284** (1999) 1340–1344

[4] J. Weissmüller, R. N. Viswanath, D. Kramer, R. Würschum and H. Gleiter. Science **300** (2003) 312–315

[5] D. Kramer, R. N. Viswanath, J. Weissmüller. Nano Letters **4**(5) (2004) 793–796

[6] J. Biener, A. Wittstock, L. A. Zepeda-Ruiz, M. M. Biener, V. Zielasek, D. Kramer, R. N. Viswanath, J. Weissmüller, M. Bäumer, A. V. Hamza. *Surface-chemistry-driven actuation in nanoporous gold*. Nature Mater., **8** (2009) 47.

[7] J. N. Barisci, G. M. Spinks, G. G. Wallace, J. D. Madden, R. H. Baughman. Smart Mater. Struct. **12** (2003) 549–555

[8] R. H. Baughman, A. A. Zakhidov, W. A. de Heer. Science **297** (2002) 787–792

[9] S. Liu, Y. Liu, H. Cebeci, R. Guzmán de Villoria, J.-H. Lin, B. L. Wardle, Q. M. Zhang. Adv. Funct. Mater. **2010**, 20, 3266–3271

[10] J. Liang, Y. Huang, J. Oh, M. Kozlov, D. Sui, S. Fang, Ray H. Baughman, Y. Ma, Y. Chen. Adv. Funct. Mater., DOI: 10.1002/adfm.201101072

[11]X. Xie, L. Qu, C. Zhou, Y. Li, J. Zhu, H. Bai, G. Shi, L. Dai. An Asymmetrically Surface-Modified Graphene Film Electrochemical Actuator. ACS Nano, 4 (2010) 6050

[12] Elzbieta Frackowiak, Review: Carbon materials for the electrochemical storage of energy in capacitors _Carbon_39_937(2001)

[13] A. Soffer and M. Folman. J. Electroanal. Chem. **38**(1) (1972) 25–43

[14] Y. Oren, I. Glatt, A. Livnat, O. Kafri and A. Soffer. J. Electroanal. Chem. **187**(1) (1985) 59–71

[15] Y. Oren and A. Soffer. J. Electroanal. Chem. **206**(1-2) (1986) 101–114

[16] D. Golub, Y. Oren and A. Soffer. J. Electroanal. Chem. **227**(1-2) (1987) 41–53

[17] D. Golub, Y. Oren, A. Soffer. Carbon **25**(1) (1987) 109–117

[18] D. Golub, A. Soffer and Y. Oren, . J. Electroanal. Chem. **260**(2) (1989) 383–392

[19] L.-H. Shao, J. Biener, D. Kramer, R. N. Viswanath, T. F. Baumann, A. V. Hamza, J. Weissmüller. *Electrocapillary maximum and potential of zero charge of carbon aerogel*. Phys. Chem. Chem. Phys., **12** (2010) 7580.

[20] T. F. Baumann, M. A. Worsley, T. Y. Han, and J. H. Satcher, Jr. "High Surface Area Carbon Aerogel Monoliths with Hierarchical Porosity", *Journal of Non-Crystalline Solids*, **2008**, *354, 3513*.

[21] F-M. Kong, J. D. LeMay, S. S. Hulsey, C. T. Alviso, and R. W. Pekala. J. Mater. Res., Vol. 8, No. 12, Dec 1993. 3100-3105

[22] Saliger, R.; Fischer, U.; Herta, C.; Fricke, J. *J. Non-Cryst Solids* **1998**, *225*, 81.

[23] Yang, K. L.; Ying, T. Y.; Yiacoumi, S.; Tsouris, C.; Vittoratos, E. S. *Langmuir* **2001**, *17*, 1961.

[24] Pekala, R. W.; Farmer, J. C.; Alviso, C. T.; Tran, T. D.; Mayer, S. T.; Miller, J. M.; Dunn, B. *J. Non-Cryst Solids* **1998**, *225*, 74.

[25] Jin, H.-J., Weissmüller, J., A material with electrically tunable strength and flow stress, Science 332 (2011) 1179-1182.
[26] K.L. Yang, S. Yiacoumi, C. Tsouris. Journal of Electroanalytical Chemistry **540** (2003) 159.

[27] G. Sun, M. Kertesz, J. Kürti, R. H. Baughman. Phys. Rev. B, 68, 125411 (2003)

[28] M. Verissimo-Alves, B. Koiller, H. Chacham, R. B. Capaz. Phys. Rev. B, 67, 161401(R)2003

[29] G. Sun, J. Kürti, M. Kertesz, R. H. Baughman. J. AM. CHEM. SOC., 2002, 124, 15076-15080

[30] G. W. Rogers, J. Z. Liu. Graphene actuators: quantum-mechanical and electrostatic double-layer effects. J. Am. Chem. Soc. 2011, 133, 10858–10863

[31] H.-J. Jin, X.-L. Wang, S. Parida, K. Wang, M. Seo, J. Weissmüller. *Nanoporous Au-Pt alloys as large strain electrochemical actuators*. Nano Lett., **10** (2010) 187.

[32] Q. Zhang, V. Bharti, X. Zhao. Giant electrostriction and relaxor ferroelectric behavior in electron-irradiated poly (vinylidene fluoride-trifluoroethylene) copolymer. Science, **280** (1998) 2101.

[33] D. R. Lide (Editor-in-Chief) CRC Handbook of Chemistry and Physics. Taylor and Francis Group, CRC press. 2008

[34]http://ilthermo.boulder.nist.gov/ILThermo/pureprp.uix.do?event=sort&source=pureindexilView133&value=Name

[35] Y. H. Yun, V. Shanov, Y. Tu, M. J. Schulz, Se. Yarmolenko, S. Neralla, J. Sankar, S. Subramaniam. A multi-*wall carbon nanotube tower electrochemical actuator*. Nano Lett., **6** (2006**)** 689.

[36] O. B. Kulyasova, R. K. Islamgaliev, R. Z. Valiev. *On the specific features of tensile tests of small samples of nanostructured materials*. Phys. Met. Metallogr., **100** (2005) 83.

[37] M. Krzesińska, A. Celzard, J.F. Marêché, and S. Puricelli. Elastic properties of anisotropic monolithic samples of compressed expanded graphite studied with ultrasounds. J. Mater. Res., **16** (2001)

[38] V. Palmre, E. Lust, A. Jänes, M. Koel, A.-L. Peikolainen, J. Torop, U. Johansona, A. Aabloo. Electroactive polymer actuators with carbon aerogel electrodes. J. Mater. Chem. 21 (2011) 2577

[39] M.M. Brunoa, N.G. Cotellaa, M.C. Mirasa, T. Kochb, S. Seidlerb, C. Barbero. Colloids and Surfaces A: Physicochem. Eng. Aspects, 358 (2010) 13–20

[40] C. Balzer, Timo W., S. Braxmeier, G. Reichenauer, J. P. Olivier. Langmuir, 2011, 27, 2553–2560

[41] R. Pelrine, R. Kornbluh, Q. Pei, J. Joseph. High-speed electrically actuated elastomers with strain greater than 100%. Science, 287 (2000) 836.

[42] J. D. W. Madden, B. Schmid, M. Hechinger, S. R. Lafontaine, P. G. A. Madden, F. S. Hover, R. Kimball, I. W. Hunter. *Application of polypyrrole actuators: feasibility of variable camber foils*. IEEE J. Oceanic Eng., **29** (2004) 706.

[43] H.-J. Jin, S. Parida, D. Kramer, J. Weissmüller. *Sign-inverted surface stress-charge response in nanoporous gold*. Surf. Sci., **602** (2008) 3588.